*Am J Physiol Regul Integr Comp Physiol* 311: R779–R787, 2016.
First published August 24, 2016; doi:10.1152/ajpregu.00243.2016.

# Antilipolytic and antilipogenic effects of the CPT-1b inhibitor oxfenicine in the white adipose tissue of rats

**Diane M. Sepa-Kishi, Michelle V. Wu, Abinas Uthayakumar, Arta Mohasses, and Rolando B. Ceddia**
*School of Kinesiology and Health Science, York University, Toronto, Ontario, Canada*

Submitted 7 June 2016; accepted in final form 17 August 2016

**Sepa-Kishi DM, Wu MV, Uthayakumar A, Mohasses A, Ceddia RB.** Antilipolytic and antilipogenic effects of the CPT-1b inhibitor oxfenicine in the white adipose tissue of rats. *Am J Physiol Regul Integr Comp Physiol* 311: R779–R787, 2016. First published August 24, 2016; doi:10.1152/ajpregu.00243.2016.—Oxfenicine is a carnitine-palmitoyl transferase 1b (CPT-1b)-specific inhibitor that has been shown to improve whole body insulin sensitivity while suppressing fatty acid (FA) oxidation and increasing circulating FA. Because the white adipose tissue (WAT) is an organ that stores and releases FAs, this study investigated whether oxfenicine-induced inhibition of FA oxidation affected adiposity and WAT metabolism in rats fed either low (LF) or high-fat (HF) diets. Following 8 wk of dietary intervention, male Sprague-Dawley rats were given a daily intraperitoneal injection of oxfenicine (150 mg/kg body wt) or vehicle (PBS) for 3 wk. Oxfenicine treatment reduced whole body fat oxidation, body weight, and adiposity, and improved insulin sensitivity in HF-fed rats. All of these effects occurred without alterations in food intake, energy expenditure, and ambulatory activity. In vivo oxfenicine treatment reduced FA oxidation and lipolysis in subcutaneous inguinal (SC Ing) adipocytes, whereas glucose incorporation into lipids (lipogenesis) was significantly reduced in both SC Ing and epididymal (Epid) adipocytes. In summary, our results show that oxfenicine-induced inhibition of CPT-1b markedly affects WAT metabolism, leading to reduced adiposity through a mechanism that involves reduced lipogenesis in the SC Ing and Epid fat depots of rats.

fatty-acid oxidation; subcutaneous and visceral fat; insulin resistance; lipolysis and fatty acid metabolism; CPT-1b inhibition

OBESITY IS A PREVALENT METABOLIC disorder and major risk factor for Type 2 diabetes (T2D). In this context, strategies to prevent the development of insulin resistance and progression to T2D are of great therapeutic interest. Many theories exist attempting to mechanistically link obesity and T2D and identify appropriate targets for intervention, one of which is the Randle cycle of substrate interaction (21). The Randle cycle proposed that the increases in mitochondrial acetyl-CoA, NADH:$NAD^+$ ratio, and citrate that occur with increased fatty acid uptake and oxidation are responsible for inhibiting key enzymes and transporters involved in glucose oxidation and uptake (21). On the basis of this theory, it was hypothesized that inhibiting fatty acid oxidation would result in an increase in glucose uptake and oxidation. While it may seem counterintuitive to decrease rates of fatty acid oxidation in a state of obesity in which fat is abundant, studies have attributed the development of insulin resistance to an overload of fatty acid oxidation and have shown that decreasing it through genetic manipulation prevents the declines seen in insulin sensitivity (15). The concern was that inhibition of β-oxidation would lead to an accumulation of lipid derivatives, such as diacylglycerol (DAG) and ceramides in skeletal muscle, which have been previously shown to contribute to the development of insulin resistance (12, 29). However, beneficial effects of reduced β-oxidation have been reported, despite intracellular accumulation of DAG and ceramides (28, 30).

Reductions in fatty acid oxidation have been achieved through the inhibition of carnitine-palmitoyl transferase-1 (CPT-1). CPT-1 is the rate-controlling enzyme for mitochondrial β-oxidation, facilitating the import of long-chain (>12C) fatty acids (LCFAs) into the mitochondria (3). Located on the outer mitochondrial membrane, CPT-1 catalyzes the reaction between long-chain acyl-CoAs and carnitine to form acylcarnitine, which is then shuttled via the carnitine acylcarnitine translocase into the mitochondria, converted back into acyl-CoA (by CPT-2), and then released to undergo β-oxidation (3). Three isoforms of CPT-1 exist: liver (CPT-1a), heart and skeletal muscle (CPT-1b), and brain (CPT-1c) (3, 22).

Oxfenicine [*S*-2-(4-hydroxyphenyl)glycine] is considered a CPT-1b-specific inhibitor. It must be transaminated to its active form, 4-hydroxyphenylglyoxylate (4-HPG), which is competitive with carnitine, preventing the formation of acylcarnitines (23). Because CPT-1b shows the highest sensitivity to 4-HPG (23), inhibition of fatty acid oxidation by oxfenicine takes place selectively in those tissues that express this CPT isoform (3). Skeletal muscle, heart, and white and brown adipose tissues are the ones with the highest content of CPT-1b in the body (3). Therefore, these tissues are expected to be the ones most responsive to oxfenicine-induced inhibition of LCFA oxidation. The effects of oxfenicine in skeletal muscle have been studied and show positive metabolic outcomes. High-fat (HF)-fed mice given daily oxfenicine injections for 14 days had a reduced area under the curve for glycemia following a glucose tolerance test compared with HF-fed control animals, indicating an improvement in whole body insulin sensitivity (14). Further analysis of the gastrocnemius muscle revealed an increased phosphorylated Akt to total Akt ratio, as well as an increase in GLUT 4 content (14).

An additional metabolic outcome of inhibiting fatty acid β-oxidation is an increase in circulating nonesterified fatty acids (NEFAs), which must find an alternate metabolic fate to oxidation. In this context, we hypothesized that the adipose tissue would undergo metabolic changes to accommodate and adjust for these excess nonoxidized fatty acids. It could do so by reducing its rates of lipolysis to prevent the further release of NEFAs, and/or by increasing rates of lipogenesis to promote the storage of excess fatty acids as triacylglycerols. These, however, have never been previously investigated. Additionally, since the adipose tissue itself also expresses CPT-1b (3), pharmacological inhibition could also have direct effects on lipid metabolism in this tissue. Importantly, metabolic differ-

Address for reprint requests and other correspondence: R. B. Ceddia, School of Kinesiology and Health Science-York Univ., 4700 Keele St., North York, ON, Canada M3J 13P3 (e-mail: roceddia@yorku.ca).

  

ences clearly exist between the visceral (e.g., epididymal, Epid) and the subcutaneous (SC) (e.g., SC inguinal, SC Ing) fat depots. The SC depot is considered to be metabolically protective (27) and more likely to change its metabolic function under various physiological conditions (7). However, it is currently unknown whether visceral and SC fat depots elicit distinct metabolic responses upon CPT-1b inhibition. Importantly, it has also been shown that oxidative capacity differs between the two depots (4, 11), which could significantly affect the response to inhibition of β-oxidation. Our study is the first to examine the in vivo and in vitro effects of oxfenicine-induced CPT-1b inhibition on adipocyte metabolism. We provide novel evidence that CPT-1b inhibition causes fat depot-specific adaptive metabolic responses that affect lipolysis, lipogenesis, and adiposity in rats.

## MATERIALS AND METHODS

*Reagents.* Type II collagenase, isoproterenol, fatty acid-free BSA, palmitic acid, oxfenicine (4-hydroxy-L-phenylglycine), and free glycerol determination kit were obtained from Sigma (St. Louis, MO). [1-$^{14}$C] palmitic acid was from American Radiolabeled Chemicals (St. Louis, MO) and D-[U-$^{14}$C]glucose was from GE Healthcare Radiochemicals (Quebec City, QC, Canada). Protease (Complete Ultra Tablets) and phosphatase (PhosphoStop) inhibitors were from Roche Diagnostics (Mannheim, Germany). The NEFA kit was from Wako Chemicals (NEFA-HR kit, Richmond, VA).

*Animals.* Male albino rats (Sprague-Dawley strain) aged 50–55 days and weighing ~250 g (upon commencement of the diet) were housed individually at 22°C on a 12:12-h light-dark cycle and fed for 11 wk ad libitum either a low-fat (LF) (Control, 27%, 13%, and 60% of calories provided by protein, fat, and carbohydrates, respectively, energy density 3.43 kcal/g), or a high-fat (HF) diet [20%, 60%, and 20% of calories provided by protein (casein), fat (lard, soybean oil), and carbohydrates (amylodextrin/sucrose), respectively, energy density 5.24 kcal/g]. The LF control diet (standard chow catalog no. 5012) was purchased from LabDiet (St. Louis, MO) and the HF diet (cat. no. D12492) was purchased from Research Diets (New Brunswick, NJ). Food intake and body weight were measured for 2 wk prior to and every day during the oxfenicine treatment. At the end of treatment, animals were placed in the Comprehensive Laboratory Animal Monitoring System (CLAMS) from Columbus Instruments for 24 h for the measurement of in vivo metabolic parameters. The animals were allowed to acclimatize for 1 h prior to collection of data, as previously described (2). The protocol containing all animal procedures described in this study was specifically approved by the Committee on the Ethics of Animal Experiments of York University [York University Animal Care Committee (YUACC) permit no. 2012-03] and performed strictly in accordance with the YUACC guidelines. All surgery was performed under ketamine/xylazine anesthesia, and all efforts were made to minimize suffering.

*In vivo treatment with oxfenicine.* Following 8 wk of either LF or HF diets, rats were given a daily intraperitoneal injection of oxfenicine (150 mg/kg body wt) suspended in 1× PBS, or just PBS (control) for three consecutive weeks.

*Determination of fasting plasma NEFAs and insulin and the procedure for the glucose tolerance test.* Following treatment with oxfenicine (*week 11*), the animals were fasted overnight, and blood was collected by saphenous vein bleeding. The animals were then intraperitoneally injected with a 20% glucose solution (2 g/kg body wt), and saphenous blood samples were taken at 15, 30, 60, and 120 min postinjection. Glucose was measured by the glucose oxidase method using a OneTouch Ultra Mini monitor. Aliquots of blood were centrifuged for 10 min at 4°C, and plasma was stored at −80°C for subsequent analysis of NEFAs and insulin.

*Adipocyte isolation.* Animals were anesthetized (0.4 mg ketamine and 8 mg xylazine per 100 g body wt) in the fed state. Subcutaneous inguinal (SC Ing) and Epid fat pads were extracted and weighed. A sample of each fat pad was immediately frozen in liquid nitrogen and stored at −80°C for subsequent Western blot analysis. The remaining tissue was used for adipocyte isolation, as described previously (11). Briefly, the adipose tissue was finely minced in Krebs-Ringer buffer (0.154 M NaCl, 0.154 M KCl, 0.11 M $CaCl_2$, 0.154 M $MgSO_4$, 0.154 M $KH_2PO_4$, and 0.154 M $NaHCO_3$, pH 7.4) with 5.5 mM glucose and 30 mM HEPES (KRBH) supplemented with type II collagenase (1 mg/ml). The finely minced tissues were then incubated at 37°C with gentle agitation (120 orbital strokes/min) for ~30–45 min. Digested tissue was strained using a nylon mesh, and cells were transferred to 50-ml tubes, carefully washed three times and resuspended in KRBH containing 3.5% BSA (KRBH-3.5% BSA). To distribute an equal number of adipocytes in each treatment condition, cell diameters and numbers were measured, as described by DiGirolamo and Fine (5).

*Determination of adipocyte lipolysis.* Lipolysis was measured by incubating adipocytes ($5 \times 10^5$ cells) either in the absence or presence of isoproterenol (100 nM). Triplicates for each condition were used, and the isolated adipocytes were incubated for 75 min at 37°C with gentle agitation (50 orbital strokes/min). Isoproterenol was used to stimulate lipolysis by acting as a nonspecific β-adrenergic agonist (1). After incubation, a 200-μl aliquot of media was taken for the determination of glycerol concentration.

*Measurement of palmitate oxidation in adipocytes.* Adipocyte oxidative capacity was assessed, as previously described, by measuring the production of $^{14}CO_2$ (11). Briefly, $2.5 \times 10^5$ cells were incubated in KRBH-3.5% BSA containing 0.2 μCi/ml of [1-$^{14}$C]palmitic acid and 200 μM nonlabeled palmitate for 1 h. The vials used for incubation had a centered well containing a loosely folded piece of filter paper. After the 1-h incubation period, the filter paper was moistened with 0.2 ml of 2-phenylethylamine/methanol (1:1, vol/vol), and the media were acidified with 0.2 ml of $H_2SO_4$ (5N). The flasks were maintained sealed at 37°C for an additional 1 h for the collection of $CO_2$ released from the cells and the media. At the end of the incubation, the filter paper was removed and transferred to a scintillation vial for radioactivity counting (8, 10).

*Western blot analysis of content and phosphorylation of proteins.* Adipose tissue collected from the Epid and SC Ing depots was homogenized in a buffer containing 25 mM Tris·HCl, 25 mM NaCl (pH 7.4), 1 mM $MgCl_2$, 2.7 mM KCl, 1% Triton-X, and protease and phosphatase inhibitors (Roche Diagnostics, Mannheim, Germany). Homogenates were centrifuged, the infranatant was collected, and an aliquot was used to measure protein by the Bradford method. Samples were diluted 1:1 (vol/vol) with 2 × Laemmli sample buffer, heated to 95°C for 5 min, subjected to SDS-PAGE, and transferred to PVDF membrane. Membranes were subsequently probed with primary antibodies (1:1,000 dilution), followed by horseradish peroxidase-conjugated anti-rabbit secondary antibody (dilution of 1:2,000). β-actin was used as a loading control. Blots were visualized using chemiluminescence (Luminata forte, Millipore, Billerica, MA) and were scanned directly into an image quantification program.

*In vitro treatment of isolated adipocytes with oxfenicine.* SC Ing and Epid adipocytes were isolated, as previously described, from LF-fed rats weighing ~250 g. Following isolation, cells were incubated in various concentrations of oxfenicine for 2 h at 37°C with gentle agitation. Assays for lipolysis, palmitate oxidation, and glucose incorporation into lipids were then performed as described in these METHODS.

*Measurement of glucose incorporation into lipids in adipocytes.* Following treatment with oxfenicine, glucose incorporation into lipids in adipocytes was assessed as previously described (20). Briefly, $1 \times 10^6$ cells were incubated in KRBH-3.5% BSA (containing 5 mM glucose) with 0.5 μCi/ml of D-[U-$^{14}$C]glucose under basal or insulin-stimulated (100 nM) conditions for 1 h at 37°C. The cells were then lysed by the addition of $H_2SO_4$ (5N) and 5 ml of Dole's reagent

(40:10:1 of isopropanol, heptane and 1 M $H_2SO_4$, vol/vol/vol) was subsequently added to the vial to extract total lipids. Radioactivity of the total lipid fraction was counted and corresponds to glucose conversion to TAG (6).

*Statistical analyses.* Normality was evaluated using the Kolmogorov-Smirnov normality test. For data that passed normality, statistical analyses were assessed by one-way and two-way ANOVAs with Bonferroni post hoc test. For data that did not pass normality, statistical analyses were assessed by Kruskal-Wallis test with the Dunn multiple-comparison test or Mann Whitney *U*-test, as indicated in the figure legends. Statistical significance was set at $P < 0.05$.

## RESULTS

*Oxygen consumption, ambulatory activity, respiratory exchange ratio, and fasting plasma NEFAs.* To examine the in vivo effects of the oxfenicine treatment, animals were placed in the CLAMS for 24 h following oxfenicine treatment and their $\dot{V}O_2$, ambulatory activity, and respiratory exchange ratio (RER) were measured. Oxfenicine had no effect on $\dot{V}O_2$ (Fig. 1*A*) or ambulatory activity (Fig. 1*B*) during the light or dark cycles. Treatment with oxfenicine also had no effect on the RER of animals fed the LF diet, whereas those fed a HF diet had significantly higher RER values, particularly during the dark cycle (Fig. 1, *C* and *D*). This is indicative of the effectiveness of oxfenicine at inhibiting fatty acid β-oxidation, resulting in an increased reliance on carbohydrate oxidation. This was more pronounced during the dark cycle (1900 to 0700), when the animals were the most active and ate the most food (0.830 ± 0.00271 $\dot{V}CO_2/\dot{V}O_2$ vs. 0.796 ± 0.00244, $\dot{V}CO_2/\dot{V}O_2$, Fig. 1, *C* and *D*). Fasting plasma NEFAs were also 1.45- and 1.46-fold higher in the LF- and HF-fed animals, respectively, following 3 wk of oxfenicine treatment (Fig. 1*E*). An increase in circulating fatty acids provides further evidence of the effectiveness of the oxfenicine treatment in reducing fatty acid oxidation.

*Fasting plasma insulin and glucose tolerance test.* As expected, HF-fed animals had a 1.6-fold increase in fasting plasma insulin compared with controls, indicating that these animals were insulin resistant (Fig. 2*A*). Further analysis of the area under the curve (AUC) of the glucose tolerance test (GTT) showed that plasma glucose remained 1.3-fold higher in the HF-fed animals compared with the LF-fed controls, confirming the development of insulin resistance in HF-fed animals (Fig. 2, *B* and *C*). Oxfenicine treatment reversed the effects of the HF diet, returning fasting insulin and plasma glucose AUC levels to those seen in the control animals (Fig. 2). Oxfenicine

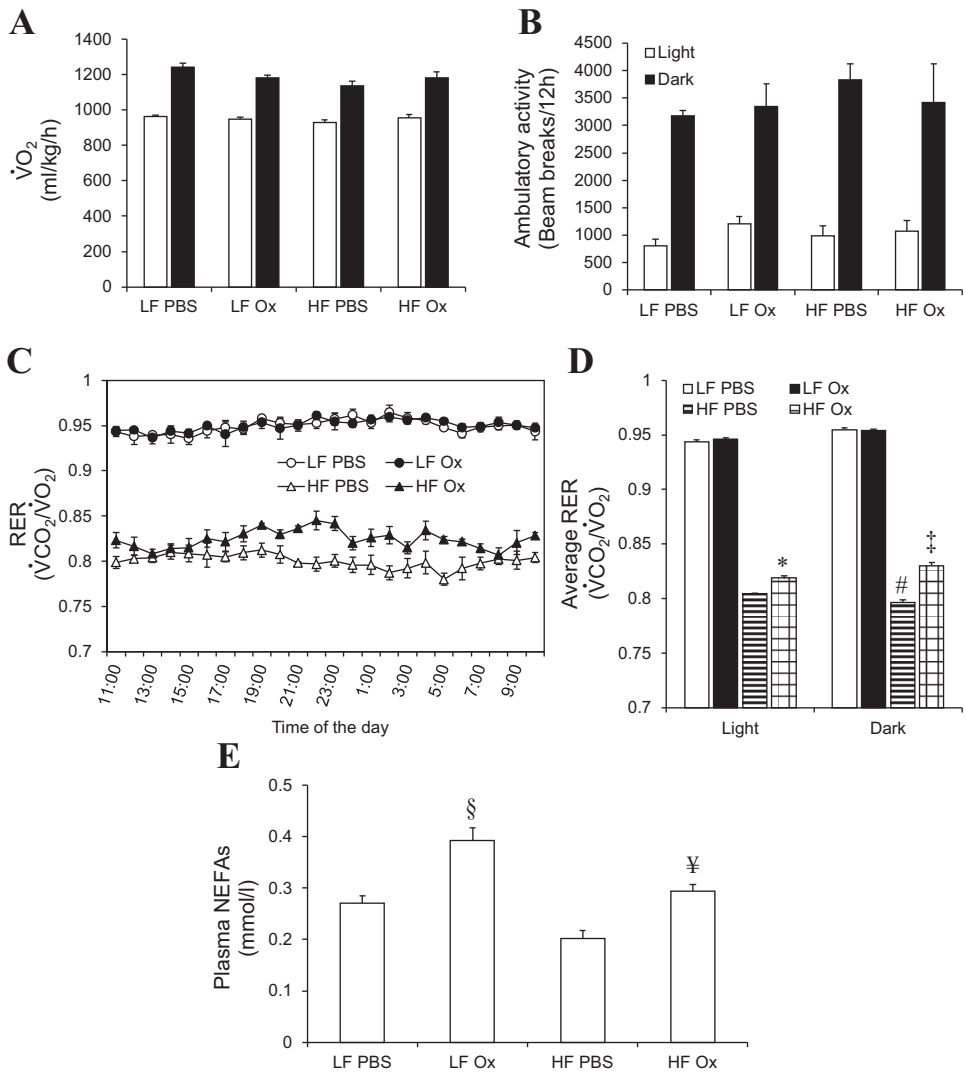


Fig. 1. Oxfenicine does not affect $\dot{V}O_2$ or ambulatory activity, but reduces whole body fat oxidation and increases circulating nonesterified fatty acids (NEFAs). The animals were fed high-fat (HF) or low-fat (LF) diets for 8 wk and then daily injected for 3 wk with either PBS (control) or oxfenicine (Ox; 150 mg/kg body wt). At the end of the oxfenicine treatment, rats were placed in the Comprehensive Laboratory Animal Monitoring System (CLAMS) for the determination of $\dot{V}O_2$ (*A*), ambulatory activity (*B*), and respiratory exchange ratio (RER) during a 24-h period (*C* and *D*). Subsequently, the animals were overnight-fasted, and blood was collected for the determination of NEFAs in the plasma (*E*). Kruskal-Wallis test, $n = 5$ for ambulatory activity. Mann-Whitney *U*-test, $n = 5$ for NEFAs. All other data were obtained by two-way analyses of variance (ANOVAS), $n = 5$. *$P < 0.05$ vs. HF PBS in the light cycle. #$P < 0.05$ vs. HF PBS light cycle. ‡$P < 0.05$ vs. HF Ox light cycle and HF PBS dark cycle. §$P < 0.05$ vs. LF PBS. ¥$P < 0.01$ vs. HF PBS.

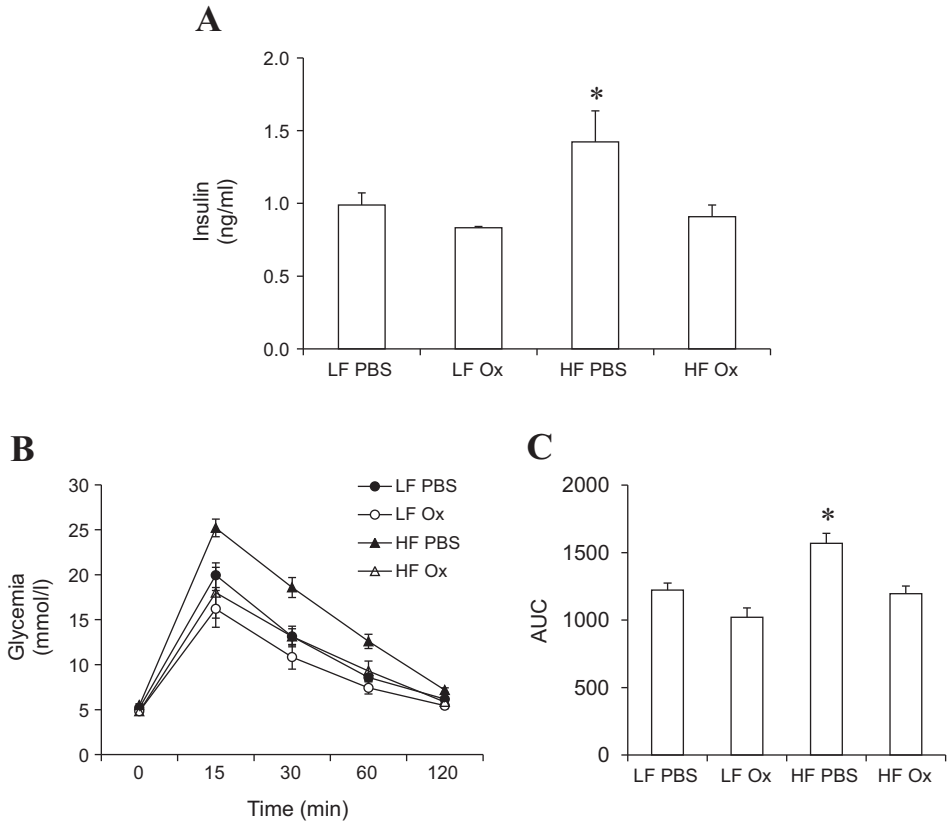


Fig. 2. Oxfenicine normalizes fasting insulin and improves insulin sensitivity. The animals were fed HF or LF diets for 8 wk and then daily injected for 3 wk with either PBS (control) or Ox (150 mg/kg body wt). *A*: at the end of the oxfenicine treatment, rats were fasted overnight, and blood was collected for the determination of insulin in the plasma. *B* and *C*: overnight-fasted rats then underwent an intraperitoneal glucose tolerance test. AUC, area under the curve. Mann-Whitney *U*-test, $n = 5$. *$P < 0.05$ vs. LF PBS and HF Ox.

treatment did not affect the glycemic response of low-fat-fed rats during the GTT.

*Body weight, food intake, and adiposity.* Energy intake during the oxfenicine treatment did not differ in the animals fed the LF (101.56 ± 5.68 vs. 94.45 ± 2.41 kcal·rat$^{-1}$·day$^{-1}$, Fig. 3*B*) or HF diet (100.40 ± 3.68 vs. 98.46 ± 4.44 kcal·rat$^{-1}$·day$^{-1}$, Fig. 3*B*). Body weight of LF-fed oxfenicine-treated rats was ~8% lower than the LF-fed PBS-treated rats (519.31 ± 9.64 g vs. 566.62 ± 24.05 g, respectively, Fig. 3*A*), although this did not reach statistical significance. However, there was a 10% significant reduction in final body weight in HF-fed animals treated with oxfenicine (Fig. 3*A*). Furthermore, oxfenicine treatment reduced Epid fat mass by 29% in the HF-fed animals (Fig. 3*C*). This effect was more pronounced in the SC Ing fat depot where oxfenicine treatment reduced fat mass by 43% and 37% in the LF- and HF-fed animals, respectively (Fig. 3*D*).

*Palmitate oxidation.* In adipocytes isolated from the Epid fat depot, palmitate oxidation was reduced in the LF-fed (0.965 ± 0.102 vs. 0.711 ± 0.056 nmol/h/2.5 × 10$^5$ cells, Fig. 4*A*) and HF-fed (1.092 ± 0.11 vs. 0.952 ± 0.101 nmol/h/2.5 × 10$^5$ cells, Fig. 4*A*) animals, although these effects were not statistically significant. This effect of oxfenicine on palmitate oxidation was more pronounced in adipocytes isolated from the SC Ing depot. In fact, palmitate oxidation in SC In adipocytes was decreased by 40% in the LF-fed animals and by 63% in the HF-fed animals (Fig. 4*B*).

*Lipolysis.* As expected, basal and isoproterenol-stimulated lipolysis differed in adipocytes isolated from the SC Ing and Epid fat depots (Fig. 5, *A* and *B*). In Epid adipocytes, there was no effect of diet or oxfenicine treatment on basal or isoproterenol-stimulated rates of lipolysis (Fig. 5*A*). However, in SC Ing adipocytes, oxfenicine treatment decreased stimulated lipolysis by 42% in the LF-fed animals (Fig. 5*B*). There was no effect of oxfenicine treatment on stimulated lipolysis in the HF-fed animals; however, the diet itself resulted in a 74% and 73% reduction in stimulated lipolysis in the HF PBS and HF Ox groups, respectively, compared with the LF-fed PBS animals (Fig. 5*B*).

*Palmitate oxidation, lipolysis, and glucose incorporation into lipids in isolated adipocytes.* In isolated adipocytes from both the Epid and SC Ing fat depots treated with 1 mM oxfenicine, palmitate oxidation was significantly reduced by 50% compared with control cells (Fig. 6, *A* and *B*). Isoproterenol-stimulated lipolysis was significantly decreased by 20% and 12% in Epid adipocytes following treatment with 100 μM and 1 mM oxfenicine, respectively (Fig. 6*C*). Similarly, in SC Ing adipocytes treatment with 100 μM and 1 mM of oxfenicine decreased stimulated lipolysis by 8% and 18%, respectively (Fig. 6*D*). There was no effect of oxfenicine on basal rates of lipolysis in Epid and SC Ing adipocytes (Fig. 6, *C* and *D*). Basal and insulin-stimulated glucose incorporation into lipids, the measure for lipogenesis, was reduced by 39% and 31%, respectively, in Epid adipocytes following treatment with 1 mM oxfenicine (Fig. 7*A*). In adipocytes from the SC Ing fat depot, the incorporation of glucose into lipids was also reduced by 41% under insulin-stimulated conditions, following 1 mM oxfenicine treatment (Fig. 7*B*).

*Adipose triglyceride lipase content and hormone sensitive lipase content and phosphorylation.* Oxfenicine treatment significantly reduced adipose triglyceride lipase (ATGL) content in the Epid adipose tissue in rats fed a LF diet (Fig. 8*A*). In the

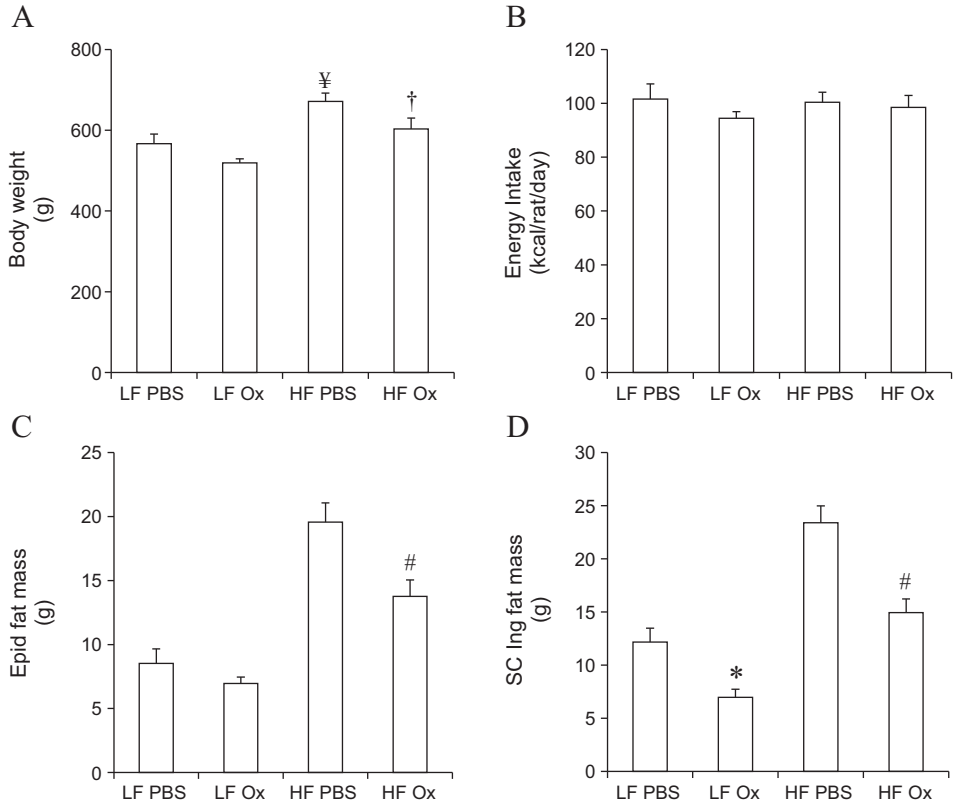


Fig. 3. Oxfenicine does not affect energy intake (*B*), but reduces body weight (*A*) and epididymal (Epid; *C*), and SC Ing (*D*) fat pad mass. Rats were fed a LF or HF diet for 8 wk and treated with either PBS or Ox (150 mg/kg body wt) for 3 wk. Kruskal-Wallis test, $n = 5$ for energy intake. All other data, two-way ANOVAs, $n = 5$. ¥$P < 0.01$ vs. LF PBS. †$P < 0.05$ vs. HF PBS and LF Ox. *$P < 0.05$ vs. LF PBS. #$P < 0.01$ vs. HF PBS.

HF-fed animals, there was no effect of oxfenicine; however, the diet itself resulted in a significant decrease in ATGL content in this fat depot (Fig. 8*A*). In contrast, ATGL content in the SC Ing adipose tissue was significantly increased with a HF diet in the PBS control animals, with no effect of oxfenicine treatment evident in rats fed either the LF or HF diet (Fig. 8*B*). There was no difference in phosphorylation of hormone sensitive lipase $(HSL)_{660}$ in either fat depot with diet or oxfenicine treatment (Fig. 8, *C* and *D*).

## DISCUSSION

Here, we report the novel findings of depot-specific alterations in adipose tissue and adipocyte metabolism following pharmacological selective inhibition of CPT-1b. The effects were characterized by a reduction in isoproterenol-stimulated lipolysis in adipocytes from the SC Ing fat depot following 3 wk of daily oxfenicine injection, indicating an increased sensitivity to oxfenicine in this fat depot. In vitro incubation of adipocytes from both fat depots with oxfenicine also resulted in a reduction in stimulated rates of lipolysis. This suggests that fat cells adjusted their metabolism to compensate for the increased circulating NEFAs seen with inhibition of β-oxidation. We also expected glucose incorporation into lipids to be increased with oxfenicine treatment to promote storage of the excess lipids, resulting from CPT-1b inhibition. Contrary to our original hypothesis, basal and insulin-stimulated glucose incorporation into lipids was significantly reduced in Epid and SC Ing adipocytes directly treated with oxfenicine. This reduction likely contributed toward sustaining elevated levels of circulating NEFAs seen in oxfenicine-treated rats. It also, at least partially, explains the decrease in Epid and SC Ing fat mass observed in oxfenicine-treated animals, as no alterations

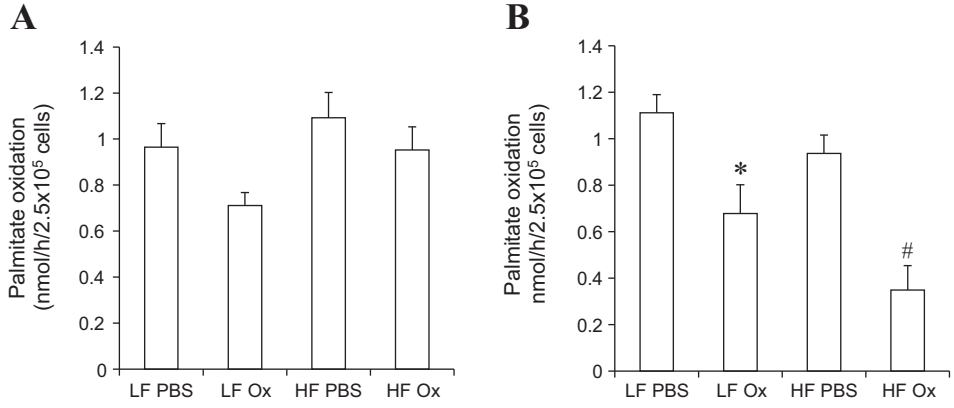


Fig. 4. Administration of oxfenicine reduces palmitate oxidation in epididymal (*A*) and subcutaneous inguinal (*B*) adipocytes. Rats were fed LF or HF diets for 8 wk and then either injected with PBS or Ox (150 mg/kg body wt) for 3 wk. Two-way ANOVAs, $n = 5$. *$P < 0.05$ vs. LF PBS. #$P < 0.01$ vs. HF PBS.

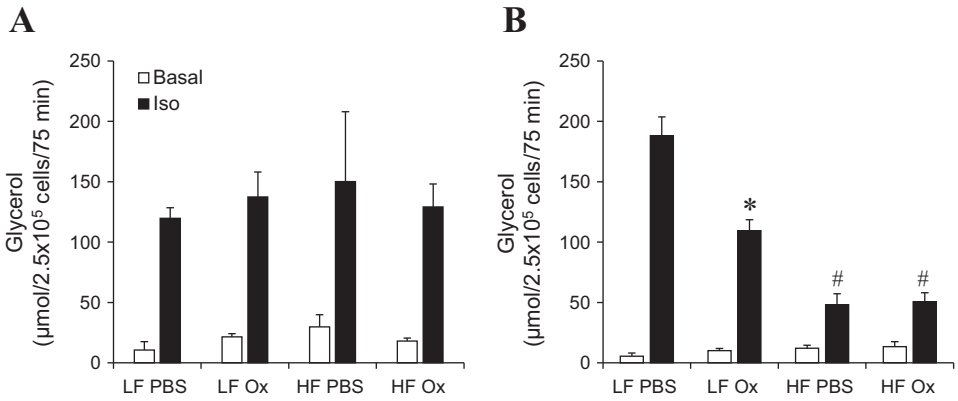


Fig. 5. Glycerol release is reduced in subcutaneous inguinal (*B*) but not in epididymal (*A*) adipocytes from LF- or HF-fed rats either injected with PBS or Ox (150 mg/kg body wt). Two-way ANOVAs, $n = 5$. *$P < 0.001$ vs. LF PBS, HF PBS, and HF Ox. #$P < 0.001$ vs. LF PBS and LF Ox.

in food intake or ambulatory activity were observed with the treatment. This suggests that reduced adiposity in oxfenicine-treated rats was mainly driven by alterations in substrate partitioning, preventing the storage of fat in the adipose tissue. This could be attributed to lower levels of the lipogenic hormone insulin in the plasma of HF-fed oxfenicine-treated rats, which is compatible with higher levels of circulating NEFAs in oxfenicine-treated rats.

Body weight of LF Ox was slightly lower (~8%) than that of LF PBS rats; however, this was not statistically different and did not characterize that rats lost weight independent of the diet following oxfenicine treatment. This could be due to the fact that in LF-fed rats treated with oxfenicine only the SC Ing fat pad was significantly reduced (43%) in its mass (Fig. 3*C*), whereas in HF-fed rats oxfenicine treatment caused a marked reduction in both Epid (29%) and SC Ing fat (37%) masses. Combining the effect of oxfenicine on Epid and SC Ing fat depots adds up to a 66% reduction in adiposity as opposed to 43% in SC Ing only in LF-fed rats. The impact of these fat depot-specific responses to oxfenicine could be the determining factor for reaching statistical significance with regard to the differences of body weight. On the basis of our findings, it appears that the effect of oxfenicine on adiposity and body weight is more evident when the organism is challenged by a HF diet, an intervention that promotes and exacerbates the accumulation of fat in the adipose tissue. Importantly, the density of adipose tissue is lower than other tissues, so a marked reduction in its content is normally required for it to exert a robust impact on total body weight. Under such conditions, the fat-reducing effect of oxfenicine seems to have caused a more pronounced effect on total body weight in HF-fed rats, and likely allowed statistical significance to be reached in this group.

The effectiveness of our pharmacological inhibition on CPT-1b was evaluated by placing the animals in the CLAMS for 24 h and measuring RER as an indication of substrate

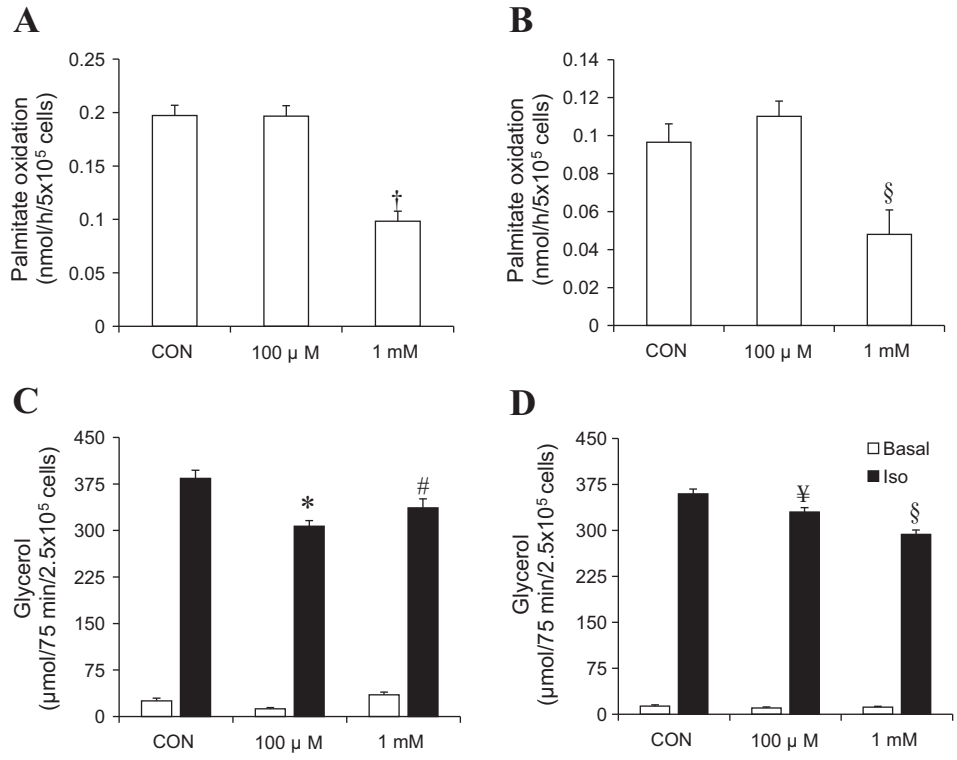


Fig. 6. Treatment with 1 mM oxfenicine reduces palmitate oxidation and isoproterenol (ISO)-stimulated lipolysis in epididymal (*A* and *C*) and subcutaneous inguinal (*B* and *D*) adipocytes. Adipocytes were extracted from lean rats and exposed to Ox (100 µM or 1 mM) in vitro for 2 h and then assayed for glycerol and palmitate oxidation. Two-way and one-way ANOVAs, $n = 5$. §$P < 0.01$ vs. CON and 100 µM. †$P < 0.0001$ vs. CON and 100 µM. *$P < 0.001$ vs. CON. #$P < 0.01$ vs. CON. ¥$P < 0.05$ vs. CON.

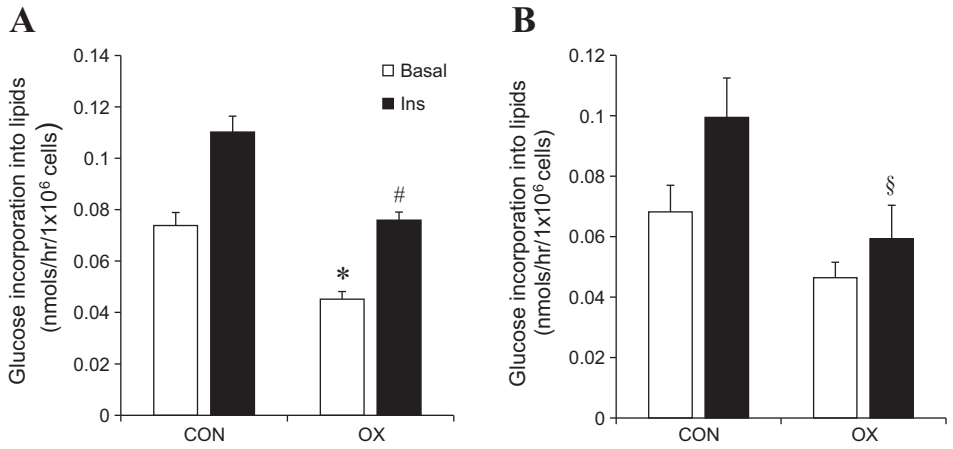


Fig. 7. Oxfenicine reduces glucose incorporation into lipids in epididymal (*A*) and subcutaneous inguinal (*B*) adipocytes. Adipocytes were extracted from lean rats and exposed to Ox (1 mM) in vitro for 2 h and then assayed for glucose incorporation into lipids. Two-way ANOVAs, $n = 5$. *$P < 0.001$ vs. Con Bas. #$P < 0.001$ vs. Con Ins. §$P < 0.05$ vs. Con Ins.

oxidation. There was a significant increase in RER in HF-fed, oxfenicine-treated animals during both the light and dark cycles, indicating a shift toward carbohydrate metabolism. Similarly to previous work (14, 30), the effect was more pronounced during the dark cycle, as this was when the animals were eating the most food and were the most active, requiring an increase in energy metabolism. Interestingly, there was no change in RER in animals fed the LF diet and treated with oxfenicine in either the light or dark cycles. Oxfenicine still seems to be exerting its inhibitory effects on β-oxidation in these animals, as plasma NEFAs are increased following treatment, to a similar extent as that seen in the HF-fed animals. It is possible that any changes in RER are masked in the LF-fed animals, as they are consuming a diet relatively low in fat that provides 60% of its energy content from carbohydrates. Under such conditions, carbohydrate is the main substrate for oxidation, so inhibition of fat oxidation does not affect RER in these animals. $\dot{V}O_2$ and ambulatory activity were also measured in vivo in the CLAMS and was not different between any of the groups, suggesting that these variables did not have an effect on the RER and adiposity data.

Previous studies examining the effects of CPT-1b inhibition have focused mainly on the metabolic improvements in skeletal muscle in animals fed a HF diet. Keung et al. (14) treated HF-fed mice with daily injections of oxfenicine for 4 wk, which resulted in an increase in the phosphorylated Akt:total Akt ratio, as well as an increase in GLUT 4 content in the gastrocnemius muscle. This was accompanied by a reduction

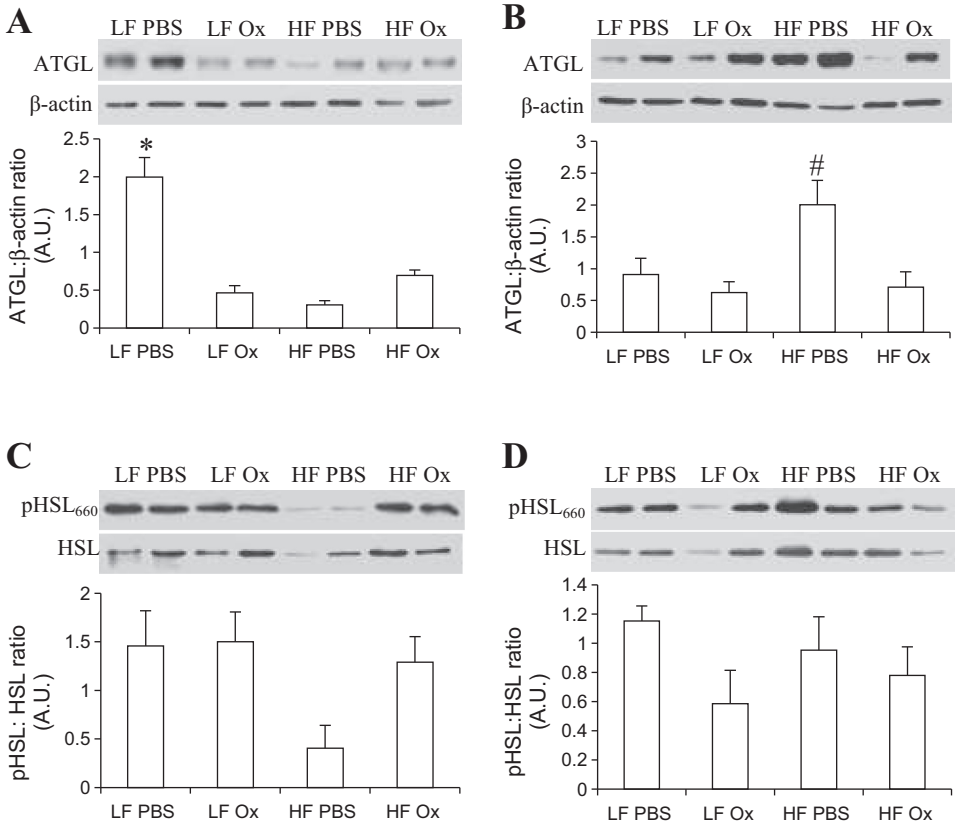


Fig. 8. Effects of oxfenicine on content of ATGL and content and phosphorylation of hormone sensitive lipase (HSL) in epididymal (*A* and *C*) and subcutaneous inguinal (*B* and *D*) adipose tissue. Animals were fed either a LF or HF diet for 8 wk, followed by 3 wk of treatment with PBS or Ox (150 mg/kg body wt). Mann-Whitney *U*-test; $n = 3$. *$P < 0.05$ vs. LF Ox and HF PBS. #$P < 0.05$ vs. all other groups.

in AUC for glycemia following a glucose tolerance test (14). Treatment of HF-fed mice with daily injections of etomoxir, a broad CPT-1 inhibitor, for 8 days has also been reported to improve whole body glucose tolerance, an effect that was accompanied by increases in phosphorylated Akt and in GLUT 4 content in the tibialis anterior muscle of mice (28). Similar to this work, we also observed a reduction in glucose AUC following a GTT in our HF-fed, oxfenicine-treated animals. This was accompanied by a reduction in fasting insulin levels, indicating an overall improvement in whole body insulin sensitivity. The effects of fatty acid inhibition on the insulin signaling pathway and whole body insulin sensitivity are likely secondary to increases in skeletal muscle glucose oxidation, as has been observed in numerous studies (17, 18, 21). In addition to the beneficial effects on glucose metabolism, we also found that oxfenicine treatment reduced body weight and adiposity in HF-fed animals. This is in line with data from Wicks et al. (30) in which a reduction in body weight and adiposity was reported in mice with muscle-specific deletion of CPT1b ($Cpt1b^{m-/-}$). Unlike our study, reduction in body weight in $Cpt1b^{m-/-}$ mice could be partially explained by a reduction in food intake (30); however, the reduction in food intake began 3–4 wk after the initial decrease in body weight and adiposity occurred, suggesting that another variable could have contributed to the decrease in weight. Our study provides evidence that a reduction in lipogenesis in the fat depots could be this alternative variable, which could at least partially explain the reduction in adiposity induced by the suppression of CPT-1b activity.

A further effect of oxfenicine treatment was the reduction in stimulated lipolysis in adipocytes isolated from the SC Ing fat depot of LF- and HF-fed animals. Stimulated lipolysis was also reduced in adipocytes that were directly treated with 1 mM oxfenicine. We expected to find a reduction in lipolysis as an adjustment made by the adipose tissue to compensate for the increased circulating NEFAs seen with CPT-1b inhibition in both LF- and HF-fed animals. The compensation makes sense physiologically, as it would prevent the further release of NEFAs into the circulation, where there is already an abundance. These NEFAs are not able to be metabolized in oxidative tissues, such as the skeletal muscle due to the CPT-1b inhibition. Despite the decrease in lipolysis, circulating NEFAs were still elevated in the oxfenicine-treated animals. This could be due to the fact that lipogenesis was also markedly inhibited in oxfenicine-treated adipocytes, which likely helped maintain elevated levels of circulating NEFAs. Importantly, chronically elevated NEFAs could result in an accumulation of lipid species in tissues such as the skeletal muscle, a condition that has been demonstrated to negatively impact insulin signaling in this tissue (13). Previous studies have, indeed, shown an increase in intramyocellular lipid and DAG contents in the skeletal muscle of the $Cpt1b^{m-/-}$ mice (30) and in animals treated with etomoxir (28). However, in both studies, there was no detrimental effect on insulin signaling. In fact, oxfenicine treatment led to an improvement in whole body glucose tolerance (28, 30). Our data are also in line with these observations, since oxfenicine treatment reduced glycemia and insulinemia in HF-fed animals to values similar to those of LF-fed controls.

Our novel results emphasize the metabolic differences between fat depots. The SC Ing fat depot has previously been shown to be metabolically protective, as it is able to store excess lipid, while remaining insulin sensitive (27). We (8, 9) and others (24, 26, 27) have demonstrated depot-specific differences in the regulation of lipolysis; however, the mechanisms underlying these differences remain poorly understood. Differences in HSL expression and activity between the SC Ing and Epid fat depots may be one possible explanation (24, 26). We were particularly interested in the regulation of ATGL, the main TAG lipase, and HSL, the main DAG lipase, in the different fat depots. The ATGL content in the Epid fat depot was significantly lower in LF-oxfenicine and HF-PBS rats compared with LF-PBS controls. However, none of these effects were accompanied by altered lipolysis in Epid adipocytes from animals either treated or nontreated with oxfenicine. In the SC Ing fat depot, the content of ATGL was increased only in the HF-fed, PBS-treated animals compared with all other groups, whereas no difference in HSL phosphorylation at serine-660 was found between any groups. ATGL is regulated by an activator, comparative gene identification-58 (16), and the full activation of both ATGL and HSL has been shown to require the phosphorylation of perilipin A (19, 25). Therefore, it is possible that lipolysis is being regulated at other proteins besides ATGL and HSL, and additional studies are required to test these possibilities.

### *Perspectives and Significance*

Chronic CPT-1b inhibition has been shown to significantly improve whole body and skeletal muscle insulin sensitivity, making it a potential obesity and T2D therapy. In our study, we present novel findings showing that oxfenicine treatment also altered lipid metabolism in adipose tissue, resulting in a reduction in fat mass in animals fed a HF diet. A daily dose of oxfenicine for 3 wk was sufficient to increase RER and circulating NEFAs. It was also accompanied by the inhibition of fatty acid oxidation in adipocytes isolated from both the Epid and SC Ing fat depots and reduced lipolysis in SC Ing adipocytes. In addition, directly treating adipocytes with oxfenicine reduced lipid storage, which must have contributed to the reduction of adiposity. To the best of our knowledge, this is the first study to examine the adaptive changes in adipose tissue metabolism that occur as a result of suppressing fatty acid oxidation through CPT-1b inhibition in vivo and provides novel additional information regarding this potential obesity and T2D therapy.

## GRANTS

This study was funded by a Discovery Grant from the Natural Sciences and Engineering Research Council of Canada (NSERC) and by infrastructure grants from the Canada Foundation for Innovation and the Ontario Research Fund awarded to R. B. Ceddia. D. M. Sepa-Kishi was supported by the Elia Scholarship and the NSERC Alexander Graham Bell Canada Graduate Scholarship.

## DISCLOSURES

No conflicts of interest, financial or otherwise, are declared by the authors.

## AUTHOR CONTRIBUTIONS

D.M.S.-K. and R.B.C. conception and design of research; D.M.S.-K., M.V.W., A.U., A.M., and R.B.C. performed experiments; D.M.S.-K., M.V.W., and R.B.C. analyzed data; D.M.S.-K. interpreted results of experiments; D.M.S.-K. prepared figures; D.M.S.-K. drafted manuscript; D.M.S.-K. and R.B.C. edited and revised manuscript; D.M.S.-K., M.V.W., A.U., A.M., and R.B.C. approved final version of manuscript.

## REFERENCES


1. **Ahlquist RP.** Present state of α- and β-adrenergic drugs I. The adrenergic receptor. *Am Heart J* 92: 661–664, 1976.
2. **Araujo RL, Andrade BM, Padrón AS, Gaidhu MP, Perry RLS, Carvalho DP, Ceddia RB.** High-fat diet increases thyrotropin and oxygen consumption without altering circulating 3,5,3′-triiodothyronine (T3) and thyroxine in rats: the role of iodothyronine deiodinases, reverse T3 production, and whole-body fat oxidation. *Endocrinology* 151: 3460–3469, 2010.
3. **Ceccarelli SM, Chomienne O, Gubler M, Arduini A.** Carnitine palmitoyltransferase (CPT) modulators: a medicinal chemistry perspective on 35 years of research. *J Med Chem* 54: 3109–3152, 2011.
4. **Deveaud C, Beauvoit B, Salin B, Schaeffer J, Rigoulet M.** Regional differences in oxidative capacity of rat white adipose tissue are linked to the mitochondrial content of mature adipocytes. *Mol Cell Biochem* 267: 157–166, 2004.
5. **DiGirolamo M, Fine JB.** Cellularity measurements. *Methods Mol Biol* 155: 65–75, 2001.
6. **DiGirolamo M.** Measurements of glucose conversion to its metabolites. In: *Methods in Molecular Biology. Adipose Tissue Protocols*, edited by Ailhaud G. Totowa, NJ: Humana Press, vol. 155, 2001, p. 181–192.
7. **Frontini A, Cinti S.** Distribution and development of brown adipocytes in the murine and human adipose organ. *Cell Metab* 11: 253–256, 2010.
8. **Gaidhu M, Anthony N.** Dysregulation of lipolysis and lipid metabolism in visceral and subcutaneous adipocytes by high-fat diet: role of ATGL, HSL, and AMPK. *Am J Physiol Cell Physiol* 298: C961–C971, 2010.
9. **Gaidhu MP, Bikopoulos G, Ceddia RB.** Chronic AICAR-induced AMP-kinase activation regulates adipocyte lipolysis in a time-dependent and fat depot-specific manner in rats. *Am J Physiol Cell Physiol* 303: C1192–C1197, 2012.
10. **Gaidhu MP, Fediuc S, Anthony NM, So M, Mirpourian M, Perry RLS, Ceddia RB.** Prolonged AICAR-induced AMP-kinase activation promotes energy dissipation in white adipocytes: novel mechanisms integrating HSL and ATGL. *J Lipid Res* 50: 704–715, 2009.
11. **Gaidhu MP, Frontini A, Hung S, Pistor K, Cinti S, Ceddia RB.** Chronic AMP-kinase activation with AICAR reduces adiposity by remodeling adipocyte metabolism and increasing leptin sensitivity. *J Lipid Res* 52: 1702–1711, 2011.
12. **Itani SI, Ruderman NB, Schmieder F, Boden G.** Lipid-induced insulin resistance in human muscle is associated with changes in diacylglycerol, protein kinase C, and IκB-α. *Diabetes* 51: 2005–2011, 2002.
13. **Jornayvaz FR, Shulman GI.** Diacylglycerol activation of protein kinase Cε and hepatic insulin resistance. *Cell Metab* 15: 574–584, 2012.
14. **Keung W, Ussher JR, Jaswal JS, Raubenheimer M, Lam VHM, Wagg CS, Lopaschuk GD.** Inhibition of carnitine palmitoyltransferase-1 activity alleviates insulin resistance in diet-induced obese mice. *Diabetes* 62: 711–720, 2013.
15. **Koves TR, Ussher JR, Noland RC, Slentz D, Mosedale M, Ilkayeva O, Bain J, Stevens R, Dyck JRB, Newgard CB, Lopaschuk GD, Muoio DM.** Mitochondrial overload and incomplete fatty acid oxidation contribute to skeletal muscle insulin resistance. *Cell Metab* 7: 45–56, 2008.
16. **Lass A, Zimmermann R, Haemmerle G, Riederer M, Schoiswohl G, Schweiger M, Kienesberger P, Strauss JG, Gorkiewicz G, Zechner R.** Adipose triglyceride lipase-mediated lipolysis of cellular fat stores is activated by CGI-58 and defective in Chanarin-Dorfman Syndrome. *Cell Metab* 3: 309–319, 2006.
17. **Li J, Stillman JS, Clore JN, Blackard WG.** Skeletal muscle lipids and glycogen mask substrate competition (Randle cycle). *Metabolism* 42: 451–456, 1993.
18. **Lillioja S, Bogardus C, Mott DM, Kennedy AL, Knowler WC, Howard BV.** Relationship between insulin-mediated glucose disposal and lipid-metabolism in man. *J Clin Invest* 75: 1106–1115, 1985.
19. **Miyoshi H, Perfield JW, Souza SC, Shen WJ, Zhang HH, Stancheva ZS, Kraemer FB, Obin MS, Greenberg AS.** Control of adipose triglyceride lipase action by serine 517 of perilipin A globally regulates protein kinase a-stimulated lipolysis in adipocytes. *J Biol Chem* 282: 996–1002, 2007.
20. **Pistor KE, Sepa-Kishi DM, Hung S, Ceddia RB.** Lipolysis, lipogenesis, and adiposity are reduced while fatty acid oxidation is increased in visceral and subcutaneous adipocytes of endurance-trained rats. *Adipocyte* 4: 22–31, 2014.
21. **Randle PJ, Garland PB, Hales CN, Newsholme EA.** The glucose fatty-acid cycle- Its role in insulin sensitivity and the metabolic disturbances of diabetes mellitus. *Lancet* 1: 785–789, 1963.
22. **Schreurs M, Kuipers F, van der Leij FR.** Regulatory enzymes of mitochondrial beta-oxidation as targets for treatment of the metabolic syndrome. *Obes Rev* 11: 380–388, 2010.
23. **Stephens TW, Higgins AJ, Cook GA, Harris RA.** Two mechanisms produce tissue-specific inhibition of fatty acid oxidation by oxfenicine. *Biochem J* 227: 651–660, 1985.
24. **Sztalryd C, Kraemer FB.** Differences in hormone-sensitive lipase expression in white adipose tissue from various anatomic locations of the rat. *Metabolism* 43: 241–247, 1994.
25. **Sztalryd C, Xu G, Dorward H, Tansey JT, Contreras AJ, Kimmel AR, Londos C.** Perilipin A is essential for the translocation of hormone-sensitive lipase during lipolytic activation. *J Cell Biol* 161: 1093–1103, 2003.
26. **Tavernier G, Galitzky J, Valet P, Remaury a Bouloumie a Lafontan M, Langin D.** Molecular mechanisms underlying regional variations of catecholamine-induced lipolysis in rat adipocytes. *Am J Physiol Endocrinol Metab* 268: E1135–E1142, 1995.
27. **Tchkonia T, Thomou T, Zhu Y, Karagiannides I, Pothoulakis C, Jensen MD, Kirkland JL.** Mechanisms and metabolic implications of regional differences among fat depots. *Cell Metab* 17: 644–656, 2013.
28. **Timmers S, Nabben M, Bosma M, van Bree B, Lenaers E, van Beurden D, Schaart G, Westerterp-Plantenga MS, Langhans W, Hesselink MKC, Schrauwen-Hinderling VB, Schrauwen P.** Augmenting muscle diacylglycerol and triacylglycerol content by blocking fatty acid oxidation does not impede insulin sensitivity. *Proc Natl Acad Sci USA* 109: 11711–11716, 2012.
29. **Ussher JR, Koves TR, Cadete VJJ, Zhang L, Jaswal JS, Swyrd SJ, Lopaschuk DG, Proctor SD, Keung W, Muoio DM, Lopaschuk GD.** Inhibition of de novo ceramide synthesis reverses diet-induced insulin resistance and enhances whole-body oxygen consumption. *Diabetes* 59: 2453–2464, 2010.
30. **Wicks SE, Vandanmagsar B, Haynie KR, Fuller SE, Warfel JD, Stephens JM, Wang M, Han X, Zhang J, Noland RC, Mynatt RL.** Impaired mitochondrial fat oxidation induces adaptive remodeling of muscle metabolism. *Proc Natl Acad Sci USA* 112: E3300–E3309, 2015.